Eur. J. Wood Prod. (2011) 69:649–657
DOI 10.1007/s00107-010-0504-0

ORIGINALS ORIGINALARBEITEN

Porosity and pore size distribution of different wood types as determined by mercury intrusion porosimetry

Michael Plötze · Peter Niemz

Received: 14 February 2010 / Published online: 27 November 2010

Abstract In this work, densities and porosity parameters are determined on domestic and overseas soft- and hardwoods by application of pycnometric methods and mercury intrusion porosimetry (MIP). Great variability was found in bulk density, porosity and in the specific surface area. According to the pore size distribution, four pore size classes could be distinguished: macropores (radius 58–2 µm and 2–0.5 µm), mesopores (500–80 nm), and micropores (80–1.8 nm). The pore size distribution can vary even in the case of comparable pore volumes. The hardwoods, particularly the European diffuse-porous ones, show a higher amount of micropores, which represent the microvoids or cell wall capillaries. A high cumulative pore volume can also be the result of a high content of micropores with poorer accessibility. The value of the total specific surface area from MIP measurements is, generally, below those values obtained by the water vapour adsorption technique. These results can provide information for further investigations on the sorption behaviour and the fluid intake as technological characteristics in industrial processes of impregnation and penetration of coating materials or adhesives.

M. Plötze (✉)
ETH Zurich, Institute for Geotechnical Engineering, ClayLab,
8093 Zurich, Switzerland
e-mail: michael.ploetze@igt.baug.ethz.ch

P. Niemz
ETH Zurich, Institute for Building Materials, Wood Physics,
8093 Zurich, Switzerland

Bestimmung der Porosität und Porengrößenverteilung verschiedener Hölzer mittels Quecksilberdruckporosimetrie

Zusammenfassung Im Rahmen der vorliegenden Arbeit wurden an ausgewählten einheimischen und überseeischen Nadel- und Laubhölzern mit pyknometrischen Methoden und der Quecksilberdruckporosimetrie verschiedene Dichte- und Porositätsparameter bestimmt. Große Unterschiede wurden in der Normal-Rohdichte, der Porosität und Porengrößenverteilung sowie in der spezifischen Oberfläche gefunden.

Anhand der Porengrößenverteilungskurven können vier Porenklassen unterschieden werden: Makroporen (Radius 58–2 µm und 2–0,5 µm), Mesoporen (500–80 nm) sowie Mikroporen (80–1,8 nm). Laubhölzer, insbesondere die untersuchten europäischen Zerstreutporigen, zeigen einen höheren Anteil an Mikroporen. Auch bei vergleichbarem totalem Porenvolumen kann die Porengrößenverteilung variieren. Ein vergleichsweise hohes kumulatives Porenvolumen kann auch durch einen hohen Anteil an Mikroporen mit niedrigerer Zugänglichkeit verursacht werden. Die aus den Daten der Druckporosimetrie bestimmte spezifische Oberfläche ist im Allgemeinen kleiner als die mittels Wasserdampfadsorption gemessene. Die vorgestellten Ergebnisse liefern Informationen für weitergehende Untersuchungen zum Sorptions- und Eindringverhalten von Flüssigkeiten in industriellen Prozessen der Imprägnierung, Beschichtung und Verklebung.

1 Introduction

Porosity and density of wood are important parameters that significantly influence material properties such as flow, adsorption and impregnability but also heat conductivity and

tensile and bending strength. Porosity is defined as one minus the solid volume fraction and can therefore, also be calculated from the normal bulk or oven-dry density ρ and the specific (or cell wall) density of solid ρ_s. There are other measuring techniques for determination of porosity of different accessibility. They are based on gas adsorption, e.g., water vapour, N_2 or He, electron microscopical investigation, and mercury intrusion porosimetry (MIP) (Lowell et al. 2004). Mercury has the advantage of not wetting most substances and not penetrating pores by capillary action. The MIP method uses pressure to force mercury into the pores, where the volume of mercury that enters the pores is related to the pore volume, and the pressure needed is related to the pore size. Measurements of the total intrusion volume, the total pore surface area, the pore size and size distribution and of the bulk and apparent specific (skeletal) density are all possible. Difficulties in the measurement of the pore size hinge on the accessibility and connectivity of the pores. Pores cannot be measured if they are closed or less than 1.8 nm radius. Therefore, the sample geometry and the measurement procedure can influence the results of pore size measurements. Mercury enters the cut cell lumina easier than the uncut ones, where the mercury has to penetrate through smaller pits at higher pressure. This can lead to an underestimation of the proportion of larger pores (cell lumina) and, consequently, an overestimation of the portion of smaller pores (Schneider and Wagner 1974). To consider this, small samples have to be used and the pressure is applied either incrementally (equilibration method) or in scanning mode continuously with a gradually increasing rate. Advanced methods allow adjusting the pressure increase rate to the pressure level and intrusion processes.

Mercury intrusion porosimetry has developed into a powerful technique to determine the pore volume and pore size distribution in many porous materials, e.g. in wood (Stayton and Hart 1965; Schneider and Wagner 1974; Schneider 1979, 1983; Hösli and Orfila 1985; Junghans et al. 2005; Pfriem et al. 2009).

Schneider (1979) investigated the pore size distribution of 30 different domestic and overseas wood species with MIP. The pore radii were classified in the ranges < 0.1 µm (diameter of margo capillaries 0.1–0.7 µm), 0.1–5 µm and >5 µm (lumen radii). The pit openings can occur in all of these radii classes. This classification was also limited by the technical capabilities of the device used (max pressure 200 MPa; min pore radius 4 nm). The investigated softwoods show only small differences in the pore size distribution mainly with pores with a radius >0.1 µm and a characteristic pore radius (average pore radius at half of the cumulative pore volume) between 1.5 and 6.0 µm. The ring-porous hardwoods mostly had pores with a radius of 0.1–5 µm and a higher ratio of small pores <0.1 µm than large pores >5 µm (e.g. Robinia 59.2%). Consequently, the average pore radius is much smaller (0.05–0.35 µm) as in softwoods. The pore size distributions of the diffuse-porous woods show wide variations but are mostly dominated by pores in the range of 0.1–5 µm. In the overseas diffuse-porous species, the characteristic pore radius is smaller than in domestic species. The lowest values (0.03 µm) were determined for Azobé and Ebony, which have the greatest quantity of small pores <0.1 µm (55.8% and 73.3%). Both woods have the highest bulk dry density (1.12–1.20 g/cm^3). However, the Doussié also has a high content of small pores <0.1 µm (60.0%) and consequently a small characteristic pore radius but still a bulk dry density of 0.837 g/cm^3. Sapwoods of larch, pine and willow, in comparison to their heartwoods, show a higher porosity and quantity of pores <5 µm. For densified solid wood (Lignostone, density 1.363 g/cm^3) and compression wood, a significantly reduced total porosity, due to fewer large pores, was found for beech (Schneider and Wagner 1974) and spruce (Schneider 1979).

Despite the importance of porosity in wood applications, there are only few systematic investigations on the porosity and pore size distribution of a wide range of different woods. Most of the studies are focused on investigating the average effective capillary radius and their effects on penetration behaviour and on the changes of the porosity of special wood types during different chemical and thermal treatments (Junghans et al. 2005; Pfriem et al. 2009). Dieste et al. (2009) investigated the pore structure of chemically (DMDHEU) modified beech with differential scanning calorimetry.

Taxonomies according to macroscopical and microscopical anatomic characteristics include the orientation and distribution of pores as well as a rough size classification (Beckwith 1997; Schoch et al. 2004). Stamm (1964) discusses the microscopic structure of wood and gives like Siau (1995), Kollmann (1987) and Wagenführ (2007) an overview of the pore structure of different woods. For softwood, the typical diameters of tracheids are between 10 and 50 µm. The almost always clogged resin ducts are in the diameter range 30–150 µm. The microvoids in the dry cell wall are found to have typical diameters of 0.3–60 nm. The effective diameter of pit openings for softwoods have been found between 0.02–4 µm. The gross structure of hardwoods is more complicated. They contain vessels with diameters in the ranges of 50–400 µm (early spring wood) and 20–50 µm (latewood). Due to these large vessel diameter the effective pore opening diameter is larger for hardwoods (5–170 µm) The lumen are in the diameter range of 1–30 µm. However, they contain also pits that are much smaller than the pits of softwoods but they are numerous and can act as alternative flow paths.

The presented work focuses on the analysis of the pore size distribution for a wide range of different wood types in

order to derive conclusions for further investigations on the sorption behaviour and the fluid intake during impregnation. The main objective is to broaden the knowledge of the pore structure.

2 Materials and methods

2.1 Wood

A series of 24 different wood types was analyzed including diffuse- and ring-porous hardwood as well as softwood (see Table 1).

Pieces were cut perpendicular to the grain in different dimensions according to the measurement needs. Each test was carried out at least in duplicate.

2.2 Density determination

The mass of air-dried (normal conditions 20°C/65% relative humidity) samples divided by their volume gives the normal bulk density ρ. The volume of the samples was determined by simply measuring the sample dimensions. Specimens of about 0.5 g weight and dimensions 20 × 6 × 6 mm were used. In the case of irregularly formed samples, the volume was determined using a pycnometer (GeoPyc 1360, MICROMERITICS) with displacement of a medium that did not intrude into the sample pores under normal pressure conditions and thus did not cause any swelling (so-called DryFlo medium, a silica nano powder).

Using the AccuPyc 1330 helium pycnometer (MICROMERITICS), the true specific gravity or cell wall density of solid ρ_s was determined. The displaced medium (helium gas) is able to fill all but the smallest micropores, thereby assuring maximum accuracy. For these measurements sawdust (size fraction 0.1–1 mm) was used to open all pores to the atmosphere. After drying the specimens (105°C), helium gas filled the sample chamber and the pressure was measured. The density is calculated with the measured volume and the known weight of the sample.

2.3 Porosity

From the oven-dry bulk density ρ and the specific solid density ρ_s, the porosity n in percent (×100) can be calculated as follows:

$$n = 1 - \frac{\rho}{\rho_s}$$

This porosity n includes all pores (open and closed). The porosity determined with mercury intrusion porosimetry only determines the percentage of open pores that are Hg-accessible. Mercury intrusion porosimetry (MIP) was carried out with a combined instrument (Pascal 140 + 440, POROTEC) for measuring macro- and mesopores in the range 58000–1.8 nm. Small isomorphous samples were used to avoid the effect of uncut pores and to eliminate anisotropic effects that may result from the cutting direction. Samples of about 0.3 g were cut perpendicular in the dimensions 5(l) × 6 (r) × 6 (t) mm. Sample sections of about 5 mm cause flow almost entirely through cut fibre cavities (Stamm 1964). First, the air dry specimens were evacuated for one hour to dry. Then the measurements were conducted by incrementing the pressure up to 400 MPa on a sample immersed in the non-wetting mercury. Hereby, the rate of pressure increase was automatically adjusted in an advanced procedure with lower rates at lower pressure levels and during measured intrusion processes. With increasing pressure, mercury intrudes into progressively smaller voids. The pore volume can be derived from the quantity of intruded mercury. The pore size distribution can be determined according to the Washburn equation, which gives a relationship between pressure and pore size (Washburn 1921).

$$r = -\frac{2\gamma \cos \Theta}{p}$$

r = pore radius, p = pressure, γ = surface tension of mercury = 0.48 N/m, Θ = wetting angle of mercury (141°, Junghans et al. 2005)

3 Results and discussion

In Table 1 the values of the normal bulk density ρ and the specific (cell wall) density ρ_s are shown. The measured specific cell wall density averages 1.493 g/cm^3 and, thus, is in good agreement with the commonly used value of 1.5 g/cm^3. The variation between all investigated different wood types is small with a minimum value of 1.458 g/cm^3 for Opepe and a maximum value of 1.528 g/cm^3 for oak. The normal bulk density is on average 0.692 g/cm^3. However, there is a significant difference between softwoods and hardwoods, with an approximately 30% lower value for softwoods (Fig. 1). The lowest bulk density was found for European spruce (0.401 g/cm^3) and the highest for Macassar ebony (1.156 g/cm^3). The diffuse-porous hardwoods show a higher variation in the bulk density. There is no obvious correlation between the normal bulk density and the cell wall density of the different wood types as claimed by Raczkowski and Stempien (1967).

The total porosity n decreases with increasing normal bulk density (Fig. 2). A possible compression of the samples due to the applied high pressure during the MIP measurements would influence the measured pore volumes. The instrument adds the compressed sample volume to the total pore volume. The practical agreement of the total porosity n with the total porosity from MIP is a sign that all the pores are open and that the pore structure did not change

Table 1 Normal bulk density, specific cell wall density and total porosity of tested species (HWdp... hardwood diffuse-porous, HWrp... hardwood ring-porous, SW... softwood)

Tab. 1 Normal-Rohdichte, Reindichte und Gesamtporosität der geprüften Holzarten. (HWdp... Laubholz zerstreutporig, HWrp... Laubholz ringporig, SW... Nadelholz)

Species trade name (German/English)	Scientific name	Type	Normal bulk density ρ g/cm^3	Specific (cell wall) density ρ_s g/cm^3	Total porosity $n = 1 - (\rho/\rho_s)$ %	Porosity (MIP) %
Bilinga/Opepe	*Nauclea diderichi* Merill.	HW dp	0.603	1.458	58.65	56.31
Bongossi/Ekki	*Lophira alata* Banks ex Gaertn. F.	HW dp	1.042	1.487	29.92	32.09
Rotbuche/Beech	*Fagus sylvatica* L.	HW dp	0.781	1.472	46.93	47.67
Buchsbaum/European boxwood	*Buxus sempervirens* L.	HW dp	0.940	1.506	37.57	37.51
Kotibé/Danta	*Nesogordonia papaverifera* Capuron	HW dp	0.698	1.480	52.82	50.71
Doussié/Afzelia	*Afzelia bipindensis* Harms	HW dp	0.826	1.501	44.98	43.30
Eibe/Yew	*Taxus baccata* L.	SW	0.626	1.481	57.74	55.66
Feldahorn/Sycamore maple	*Acer Campestre* L.	HW dp	0.483	1.512	68.05	69.69
Fichte/Norway spruce	*Picea abies* Karst.	SW	0.401	1.524	73.68	68.39
Framiré/Idigbo	*Terminalia ivorensis* A. Chev.	HW dp	0.616	1.501	58.95	51.53
Hängebirke/Common birch	*Betula pendula* Roth.	HW dp	0.594	1.502	60.45	57.12
Lärche/European Larch	*Larix decedua* Mill.	SW	0.588	1.481	60.30	57.62
Makassar-Ebenholz/Macassar ebony	*Diospyros celebica* Bakh.	HW dp	1.156	1.484	22.10	23.30
Bété/Mansonia	*Mansonia altissima* A. Chev.	HW dp	0.625	1.466	57.37	55.01
Merbau	*Intsia bijuga* O. Ktze.	HW dp	0.902	1.518	40.56	40.25
Okoumé/Gaboon	*Aucoumea klaineana* Pierre	HW dp	0.426	1.473	71.09	67.29
Ramin	*Gonystylus bancanus* Baill.	HW dp	0.608	1.505	59.59	58.62
Robinie/False acacia	*Robinia pseudoacacia* L.	HW rp	0.726	1.509	51.88	48.37
Eiche/Oak	*Quercus robur* L.	HW rp	0.706	1.528	53.81	49.09
Kiefer/Scots pine	*Pinus sivestris* L.	SW	0.451	1.489	69.71	65.40
Erle/White alder	*Alnus glutinosa* Gaertn.	HW dp	0.538	1.492	63.95	60.05
Weißes Lauan/White Lauan	*Pentacme contorta* Merr. Et. Rolfe	HW dp	0.627	1.474	57.46	48.50
Wengé	*Millettia laurentii* De Wild.	HW dp	0.930	1.482	37.24	34.17
Zebrano	*Microberlinia brazzavillensis* A. Chev.	HW dp	0.704	1.504	53.20	46.38

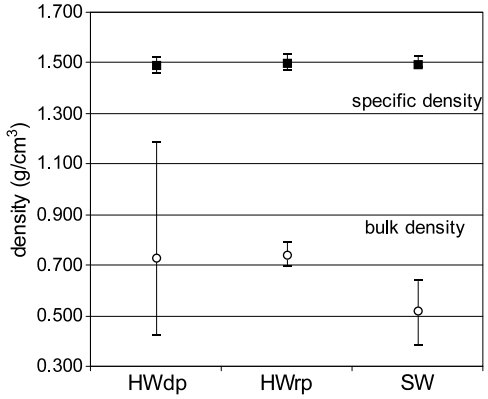

Fig. 1 Distribution of normal bulk density ρ and specific (cell wall) density ρ_s, separated in softwood and ring- and diffuse-porous hardwood (HWrp and HWdp, resp.). The *bars* mark the min and max values

Abb. 1 Verteilung von Normal-Rohdichte und Reindichte getrennt nach Nadelholz, sowie ring- und zerstreutporiges Laubholz. Die *Balken* kennzeichnen die Minimal- und Maximalwerte

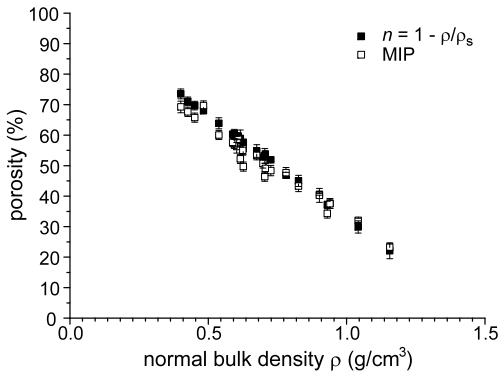

Fig. 2 Decreasing total porosity with increasing normal bulk density; agreement of the total porosity n with the total porosity from MIP (except for Idigbo, White Lauan and Zebrano)

Abb. 2 Mit zunehmender Rohdichte abnehmende Gesamtporosität

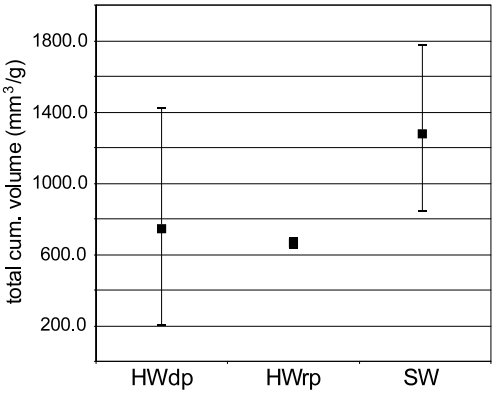

Fig. 3 Cumulative pore volume, separated in softwood and rp and dp hardwood

Abb. 3 Gesamtporenvolumen in mm^3/g getrennt nach Nadelholz, sowie ring- und zerstreutporigem Laubholz

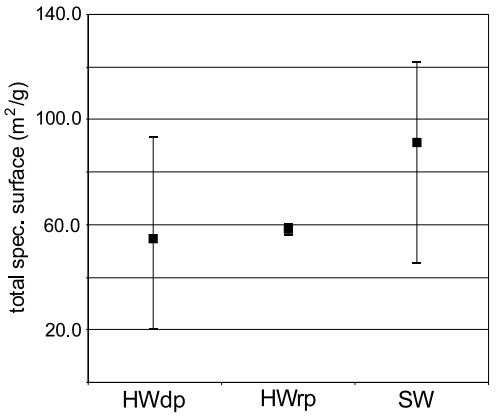

Fig. 4 Total specific surface from tested wood species, separated in softwood and rp and dp hardwood

Abb. 4 Spezifische Gesamtoberfläche der geprüften Holzarten, getrennt nach Nadelholz sowie ring- und zerstreutporigem Laubholz

during the MIP measurement (Schneider and Wagner 1974). A further check of the possible falsifying sample compression is to calculate the difference of the bulk volume (inverse of bulk density) and the solid volume (inverse of the specific cell wall density) and relate this pore volume to the measured pore volume. A higher pore volume means sample compression. The measured wood samples showed only in some cases (white lauan, Afzelia, Macassar ebony, Gaboon, beech, False acacia, Ramin, and yew) a very weak sample compression <5% of the measured cumulative pore volume.

Table 2 shows results of the MIP measurements. The cumulative pore volume is on average 821 mm^3/g. In accordance to the normal bulk density, there is a significant difference between softwood and hardwood. The hardwoods have on average 60% of the pore volume of softwoods (Fig. 3). However, there are high variations in the values. For diffuse-porous hardwoods pore volumes between 203 mm^3/g (Macassar ebony) and 1416 mm^3/g (Sycamore maple) were measured. The same is true for the total specific surface area (Fig. 4). The values vary greatly, but are generally below those that were determined with water vapour adsorption measurements using the Hailwood-Horrobin model (e.g., spruce 205 g/m^2, pine 203 g/m^2, and larch 224 m/g^2; Popper and Niemz 2009). This is due to the accessibility of water vapour in pores even smaller than 1.8 nm. According to the shape of the Volume-Pressure-Curves of the MIP (not shown) the pores in the investigated woods correspond to the spherical model (sometimes called ink bottle pores). Larger pore volumes are connected by very narrow pores. After reaching their "breakthrough pressure" the whole volume is filled very slowly. This breakthrough diameter has a direct practical meaning in impregnation processes. To avoid a shift of the measured pore radius to lower values during the measurements, the rate of pressure increase was auto-

Table 2 Pore sizes and pore size distribution of the tested species from mercury intrusion porosimetry

Tab. 2 Porengrößen und Porengrößenverteilung für die geprüften Holzarten

Species trade name (German/English)	Type	Relative pore volume in %				Most frequent pore radius nm	Characteristic pore radius nm	Cumulative pore volume mm^3/g	Total specific surface m^2/g
		Macropores		Mesopores 500–80 nm	Micropores 80–1.8 nm				
		58–2 µm	2–0.5 µm						
Bilinga/Opepe	HW dp	26.91	4.06	19.64	49.41	44.2	84.2	904.30	52.80
Bongossi/Ekki	HW dp	21.53	2.61	30.83	44.81	132.2	110.4	323.47	30.33
Rotbuche/Beech	HW dp	46.91	13.92	12.79	26.38	3856.4	1571.4	638.96	58.32
Buchsbaum/European boxwood	HW dp	5.29	17.34	6.44	70.93	10.2	11.1	422.95	38.31
Kotibé/Danta	HW dp	40.73	6.49	3.33	49.45	15.2	102.0	745.27	73.18
Doussié/Afzelia	HW dp	15.85	3.81	14.43	65.90	58.2	62.2	495.67	41.74
Eibe/Yew	SW	7.68	37.53	46.26	8.54	364.1	452.4	840.09	45.34
Feldahorn/Sycamore maple	HW dp	31.63	58.57	7.39	2.41	525.9	816.1	1415.84	71.99
Fichte/Norway spruce	SW	26.01	19.93	49.16	4.90	148.2	339.9	1770.17	117.97
Framiré/Idigbo	HW dp	35.33	5.69	31.76	27.21	87.5	178.0	771.17	63.96
Hängebirke/Common birch	HW dp	44.88	41.98	8.77	4.37	6399.1	873.5	984.54	63.01
Lärche/European Larch	SW	44.61	15.54	24.13	15.74	9557.4	1334.3	989.90	80.66
Makassar-Ebenholz/Macassar ebony	HW dp	10.32	6.24	9.48	73.95	31.2	30.2	202.58	19.98
Bété/Mansonia	HW dp	38.39	3.11	24.37	34.14	35.1	223.4	892.92	74.76
Merbau	HW dp	20.38	1.85	35.60	42.18	122.1	107.7	443.20	37.69
Okoumé/Gaboon	HW dp	4.39	19.22	18.87	57.52	43.3	57.4	1234.75	93.28
Ramin	HW dp	19.55	51.08	11.03	18.34	426.5	588.0	927.34	54.75
Robinie/False acacia	HW rp	3.51	4.57	36.33	55.59	12.6	50.3	685.71	58.58
Eiche/oak	HW rp	22.26	9.16	31.63	36.95	12.7	178.0	687.31	59.22
Kiefer/Scots pine	SW	62.90	16.45	16.15	4.50	12454.8	4044.4	1506.12	121.78
Erle/White alder	HW dp	42.16	36.94	13.64	8.27	5328.8	1062.4	1117.82	74.00
Weißes Lauan/White lauan	HW dp	21.69	3.14	45.41	29.76	158.5	174.2	593.12	46.36
Wengé	HW dp	10.43	3.76	49.84	35.96	44.7	145.0	376.85	30.07
Zebrano	HW dp	17.17	20.83	38.11	23.88	367.5	345.1	721.20	52.79

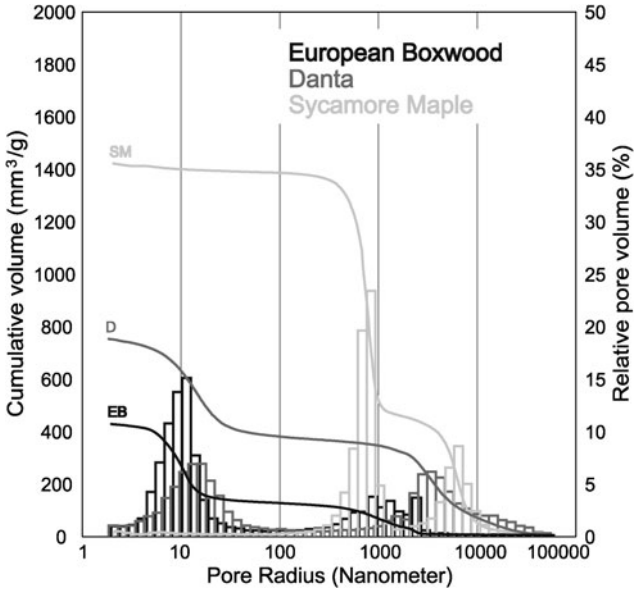

Fig. 5 Cumulative pore volume and histogram of relative pore volume as a function of the pore radius of European boxwood, Danta and Sycamore maple as examples of the different distribution types of European diffuse-porous hardwood

Abb. 5 Kumulatives Porenvolumen und Porengrößenverteilungshistogramm von Buchsbaum, Kotibé und Feldahorn als Beispiele der unterschiedlichen Typen in europäischen zerstreutporigen Laubhölzern

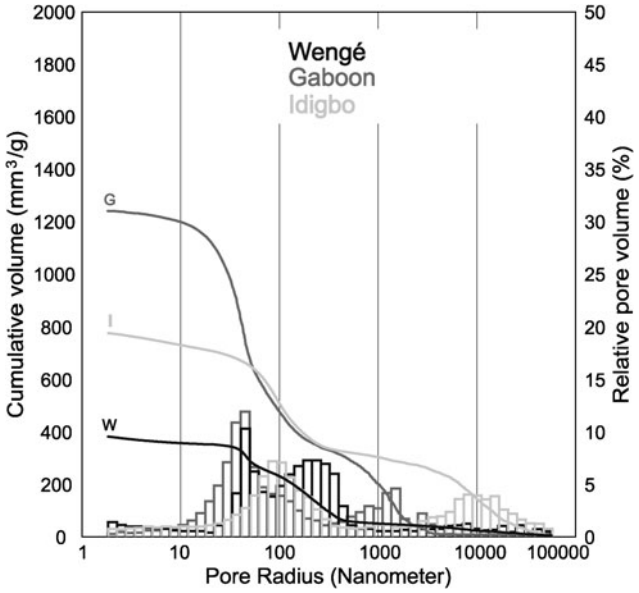

Fig. 6 Cumulative pore volume and histogram of relative pore volume as a function of the pore radius of Gaboon, Wengé and Idigbo, illustrating the different distribution types of overseas diffuse-porous hardwood

Abb. 6 Kumulatives Porenvolumen und Porengrößenverteilungshistogramm von Okoumé, Wengé und Framiré als Beispiele der unterschiedlichen Typen in überseeischen zerstreutporigen Laubhölzern

matically adjusted to very low rates at lower pressure levels and during such measured intrusion processes. Whereas the intrusion curves were rather steep, the extrusion curves were more or less flat lines because the samples retain almost completely the mercury inside the pores. The calculated surface area (Table 2) depends in this case on the pore volume only.

Figures 5–7 show examples of the different types of cumulative pore volume and pore size distributions between 1.8 nm and 58 µm. Because of technical restriction the measurement of the large tracheids with diameters >58 µm is excluded. Those pores are on the one hand important openings in impregnation but on the other hand easily accessible already without or with low applied pressures. The diffuse-porous hardwoods (Figs. 5, 6) have a bimodal pore size distribution with two clearly separated maxima. Sycamore maple has both maxima above 500 nm and conclusively the highest pore volume in hardwood. Wengé shows, like Ekki, both maxima below 500 nm and conclusively a low cumulative pore volume. Only for the overseas diffuse-porous hardwood, pores in the range of approximately 100 nm could be measured. The lowest cumulative pore volume was measured for Macassar ebony, which has only one smeared pore maxima at approximately 30 nm. The ring-porous hardwoods are characterised by pore maxima at approximately 10 nm, 200 nm and a weaker maximum at 3 µm. The semi-ring-porous beech shows a very similar distribution. The pore

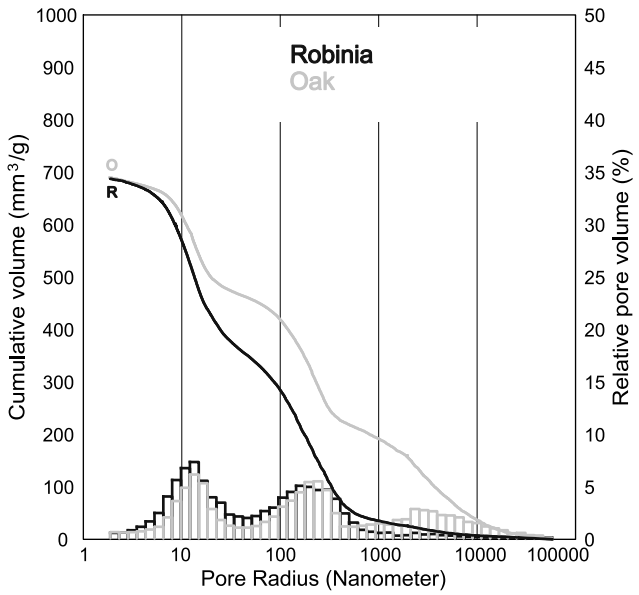

Fig. 7 Cumulative pore volume and histogram of relative pore volume as a function of the pore radius of Oak and Robinia, illustrating the different distribution types of ring-porous hardwood

Abb. 7 Kumulatives Porenvolumen und Porengrößenverteilungshistogramm von Eiche und Robinie als Beispiele der unterschiedlichen Typen in ringporigen Laubhölzern

size distribution of softwoods is widely variable between 20 µm down to 2 nm radius and shows mainly one or two maxima above 100 nm. The maximum at approximately

20 nm radius is very weak compared to the one of hardwoods.

Based on the different distribution curves, the pores are classified as micropores with a radius <80 nm, mesopores with a radius size between 500–80 nm and macropores summarising the class of pore size with a radius between 2–0.5 µm and >2 µm (Table 2). The micropores represent the microvoids or cell wall capillaries. The macropores include the lumen as well as some smaller tracheid openings. Pit openings can occur in the mesopore as well as in the macropore range. The ratio of these pore classes normalized to 100% is shown in Fig. 9. All investigated woods are distributed in the field below 50% of mesopores. The softwoods are situated in the ternary diagram at the side with a low relative content of micropores (maximum 16%; European larch). However, even with a comparable and high cumulative pore volume of Norway spruce and Scots pine, there is great variability in the relative content of macropores with lower values for yew and Norway spruce (45%) and a higher value for Scots pine (79%). The latter shows the highest content of macropores with a great maximum in the largest pores at approximately 12 µm radius (Fig. 8, Table 2).

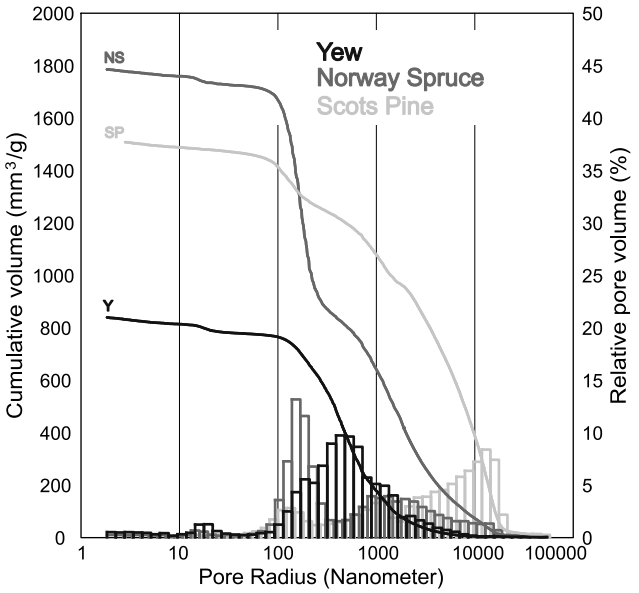

Fig. 8 Cumulative pore volume and histogram of relative pore volume as a function of the pore radius of Yew, European spruce and Scots pine, illustrating the different distribution types of softwood
Abb. 8 Kumulatives Porenvolumen und Porengrößenverteilungshistogramm von Eibe, Fichte und Kiefer als Beispiele der unterschiedlichen Typen von Nadelhölzern

Higher amounts of large pores were also found in diffuse-porous hardwoods (White alder 79%, common birch 86%, and Sycamore maple 90%). These three hardwoods are similarly characterised by two maxima in pore size distribution at approximately 700 nm and 7 µm. Ramin also has a comparable amount of macropores (71%), this is the result of a large percentage of one type of pore with a radius of 400 nm. These mentioned hardwoods are characterised by a higher cumulative pore volume. A comparable high cumulative pore volume was also measured for Gaboon and Opepe. However, this higher cumulative pore volume is caused by a high content of micropores with poorer accessibility, e.g. in impregnation processes. In the left corner of the ternary diagram with a low amount of macro and mesopores, Macassar

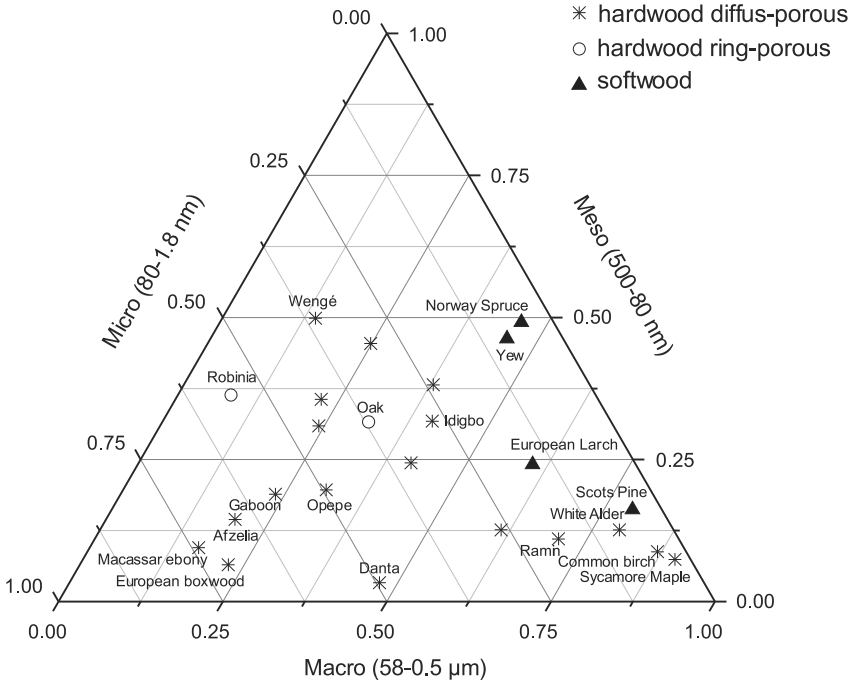

Fig. 9 Distribution of macro, micro and mesopores, separated for softwood, and rp and dp hardwood
Abb. 9 Verteilung von Makro, Mikro und Mesoporen getrennt nach Nadelholz sowie ring- und zerstreutporigem Laubholz

ebony and European Boxwood can be found with the highest relative content of micropores. These two woods possess the highest normal bulk densities. Only Robinia, a ring-porous hardwood, has a lower content of macropores but with a higher content of mesopores.

4 Conclusion

Porosity and density are important parameters that significantly influence properties of wood such as flow, adsorption and impregnability but also thermal conductivity and tensile and bending strength. The measurements of these parameters from a wide range of different wood types show significant differences in bulk density and porosity, but nearly no variations in the common value of 1.5 g/cm^3 for the cell wall density. A correlation between the normal bulk density and the cell wall density was not found. From the pore size distribution curves, four pore size ranges could be distinguished. Even at comparable cumulative pore volumes, there are differences in the relative amount of different pore sizes, particularly in the ratio of micropores and macropores. High cumulative pore volumes can also be caused by a high content of micropores, which have poorer accessibility. The value of the total specific surface area from MIP measurements is, generally, below those values achieved using the water vapour adsorption technique due to the accessibility of water vapour in pores even smaller than 1.8 nm. The results of pore size distribution can provide useful information, particularly on the fluid intake, and supply technological characteristics in industrial processes of impregnation and penetration of coating materials or adhesives.

Acknowledgements We thank Beat Hornung (ETH Zurich, Institute for Geotechnical Engineering) for help in MIP measurements.

References

Beckwith III JR (1997) Separating certain species-groups of woods for identification, based on readily visible characteristics. Warnell School of Forest Resources (Wood Products). Online version: http://warnell.forestry.uga.edu/service/library/for97-193/for97-193.html

Dieste A, Krause A, Mai C, Sébe G, Militz H (2009) Modification of *Fagus sylvatica* L with 1,3-dimethylol-4,5-dihydroxy ethylene urea (DMDHEU) Part 2: Pore size distribution determined by differential scanning calorimetry. Holzforschung 63(1):89–93

Hösli JP, Orfila C (1985) Mercury porosimetric approach on the validity of Darcy's law in the axial penetration of wood. Wood Sci Technol 19:347–352

Junghans K, Niemz P, Bächle F (2005) Untersuchungen zum Einfluss der thermischen Vergütung auf die Porosität von Fichtenholz. Holz Roh-Werkst 63(3):243–344

Kollmann F (1987) Poren und Porigkeit in Hölzern. Holz Roh-Werkst 45(1):1–9

Lowell S, Shields JE, MA Thomas, Thommes M (2004) Characterization of porous solids and powders: surface area, pore size and density. Kluwer Academic, Dordrecht

Pfriem A, Zauer M, Wagenführ A (2009) Alteration of the pore structure of spruce (*Picea abies* (L.) Karst.) and maple (*Acer pseudoplatanus* L.) due to thermal treatment as determined by helium pycnometry and mercury intrusion porosimetry. Holzforschung 63:94–98

Popper R, Niemz P (2009) Wasserdampfsorptionsverhalten ausgewählter heimischer und fremdländischer Holzarten. Bauphysik 31(2):117–121

Raczkowski J, Stempien C (1967) Zur Beziehung zwischen der Rohdichte und der Reindichte von Holz. Holz Roh-Werkst 25(10):380–383

Schneider A (1979) Beitrag zur Porositätsanalyse von Holz mit dem Quecksilber-Porosimeter. Holz Roh-Werkst 37(8):295–302

Schneider A (1983) Untersuchungen über die Eignung der Quecksilber-Porosimetrie zur Beurteilung der Imprägnierbarkeit von Holz. Holz Roh-Werkst 41(3):101–107

Schneider A, Wagner L (1974) Bestimmung der Porengrössenverteilung in Holz mit dem Quecksilber-Porosimeter. Holz Roh-Werkst 32(6):216–224

Schoch W, Heller I, Schweingruber FH, Kienast F (2004) Wood anatomy of central European Species. Online version: http://www.woodanatomy.ch

Siau JF (1995) Influence of moisture on physical properties. Department of Wood Science: and Forest Products, Virginia Tech

Stamm AJ (1964) Wood and cellulose science. Ronald Press, New York

Stayton CL, Hart CA (1965) Determining pore size distribution in softwoods with a mercury porosimeter. For Prod J 15:435–440

Wagenführ R (2007) Holzatlas. Fachbuchverlag im Carl Hanser Verlag, Leipzig

Washburn EW (1921) Note on a method of determining the distribution of pore sizes in a porous material. Proc Natl Acad Sci 7:115–116